

Coupling of field-induced spin fluctuations and spin-density wave in intermetallic CeAg₂Ge₂

D. K. Singh,^{1,2} A. Thamizhavel,³ S. Chang,¹ J. W. Lynn,¹ D. A. Joshi,³ S. K. Dhar,³ and S. Chi^{1,2}

¹NIST Center for Neutron Research, Gaithersburg, Maryland 20899, USA

²Department of Materials Science and Engineering, University of Maryland, College Park, Maryland 20742, USA

³Tata Institute of Fundamental Research, Mumbai, India

(Received 26 April 2011; published 9 August 2011)

We report on experimental evidence for a coupling between the magnetic-field-induced fluctuations of correlated Ce ions coinciding with the discontinuous movement of the underlying spin-density wave in the intermetallic rare-earth compound CeAg₂Ge₂. The measurements performed using neutron scattering and magnetic Grüneisen ratio methods suggest that the coupling is onset at $H = 2.7$ T and $T \leq 3.8$ K and persists to the lowest measurement temperature of $\simeq 0.05$ K. These measurements suggest that the spin fluctuations can affect the intrinsic properties of the system.

DOI: [10.1103/PhysRevB.84.052401](https://doi.org/10.1103/PhysRevB.84.052401)

PACS number(s): 75.30.Fv, 75.25.-j, 75.30.Kz, 74.40.Kb

Intermetallic rare-earth compounds containing a lattice of $4f$ or $5f$ electrons (such as Ce, U, and Yb) are prototypical systems to study the magnetic quantum phase transition (QPT); a second-order phase transition separating the paramagnetic state from the magnetically ordered state at $T = 0$ K.¹⁻⁴ The standard model of QPT based on the Hertz-Millis-Moriya spin-fluctuation theory invokes the idea that the QPT results from the fluctuations of the antiferromagnetic moment (order parameter) and that their intensity diverges at the QPT.⁵⁻⁷ The dynamic behavior, manifested by spin fluctuations, is experimentally probed using an external control parameter such as pressure, chemical doping, or magnetic field. While the synergistic efforts of theoretical and experimental investigations have led to a broader understanding of the mechanism behind spin fluctuations and the related scaling of the dynamic spin susceptibility, new behaviors have also emerged, especially in itinerant magnetic systems, that prohibit a universal formulation and require further experimental investigations of spin fluctuation phenomena.⁸⁻¹²

In this Brief Report, we report on the experimental investigation of a Ce-based intermetallic compound, CeAg₂Ge₂, which belongs to $I4/mmm$ tetragonal space group with lattice constants of $a = b = 4.305$ Å and $c = 10.971$ Å. The study of CeAg₂Ge₂ is interesting in itself as it exhibits an interplay of modest heavy-fermion behavior and long-range antiferromagnetic order, $T_N = 4.6$ K.^{13,14} The paramagnetic susceptibility shows an easy [100] direction in the tetragonal plane and an effective magnetic moment per Ce ion of $2.54 \mu_B$. The lack of single crystals until now has inhibited the determination of the ground-state magnetic configuration and the detailed exploration of possible critical behavior in this compound. We have performed a series of neutron scattering and magnetic Grüneisen ratio measurements on single-crystal CeAg₂Ge₂ in applied magnetic field up to 9 T. The ground-state magnetic configuration of correlated Ce ions forms a spin-density-wave (SDW) magnetic structure with Ce spins fluctuating spatially along the b axis (equivalent to a axis). However, the main result of this Brief Report is the discovery of a coupling between the moment fluctuations of correlated Ce ions, also manifested by a subtle change in the ordered moment, and the discontinuous movement of the underlying SDW configuration in applied magnetic fields along the [100] direction. It is found that while the spins fluctuate temporally along the [0K0]

direction, collectively they move along the [00L] direction in a discontinuous way at $H = 2.7$ T and $T \leq 3.8$ K. The discontinuous movement of correlated Ce spins coincides with a change in ordered moment and moment fluctuations in the H - T phase space and, hence, suggest that the localized fluctuations can induce a dynamic response to the intrinsic properties of the system.

Neutron scattering measurements were performed on a 0.5-gm single crystal of CeAg₂Ge₂ at the spin-polarized triple-axis spectrometer (SPINS) and thermal triple-axis spectrometers (BT7 and BT9) with fixed final neutron energies of 3.7 and 14.7 meV, respectively. The high quality of the single crystal was verified by means of x-ray and Laue diffraction pattern.¹⁴ The measurements at SPINS employed a flat pyrolytic graphite (PG) analyzer with collimator sequence Mono-80'-sample-BeO-80'-flat analyzer-open while the measurements on the thermal spectrometers were performed using a flat PG analyzer with collimations PG filter-Mono-50'-sample-PG filter-50'-Flat analyzer-120'. Measurements were performed with the crystal oriented in the (0KL) scattering plane and mounted in a dilution fridge with a base temperature of 50 mK. Here, K and L represent reciprocal lattice units of $2\pi/b$ and $2\pi/c$, respectively. For the magnetic field measurements, the field was applied along the easy [100] direction.

Neutron scattering measurements performed on powder form of CeAg₂Ge₂¹³ had identified magnetic reflections with a modulation vector ϵ of (0.0,0.285,0.9). Our single-crystal measurements allow for a much more detailed examination of the intensities and magnetic-scattering pattern. In Figs. 1(a) and 1(b), we plot elastic data obtained on BT7 and SPINS for representative scans at different temperatures along the K and L directions. The incommensurate peak positions, defined by $\mathbf{q} = \boldsymbol{\tau} \pm \boldsymbol{\epsilon}$, where $\boldsymbol{\tau}$ and $\boldsymbol{\epsilon}$ are the nuclear and modulation vectors, respectively, are found to be temperature independent at \mathbf{q} . As the sample is cooled below 4.5 K, resolution-limited magnetic peaks (with a lower limit of 144 unit cells) clearly develop, indicating the development of long-range magnetic order in the system.

We have performed detailed elastic scattering measurements at $T = 1.5$ K and $H = 0$ T in the (0KL) zone spanning a wide region of reciprocal space using 14.7 meV neutrons, as shown in Fig. 2(a). All four satellites of the incommensurate magnetic peaks were observed around the nuclear peak

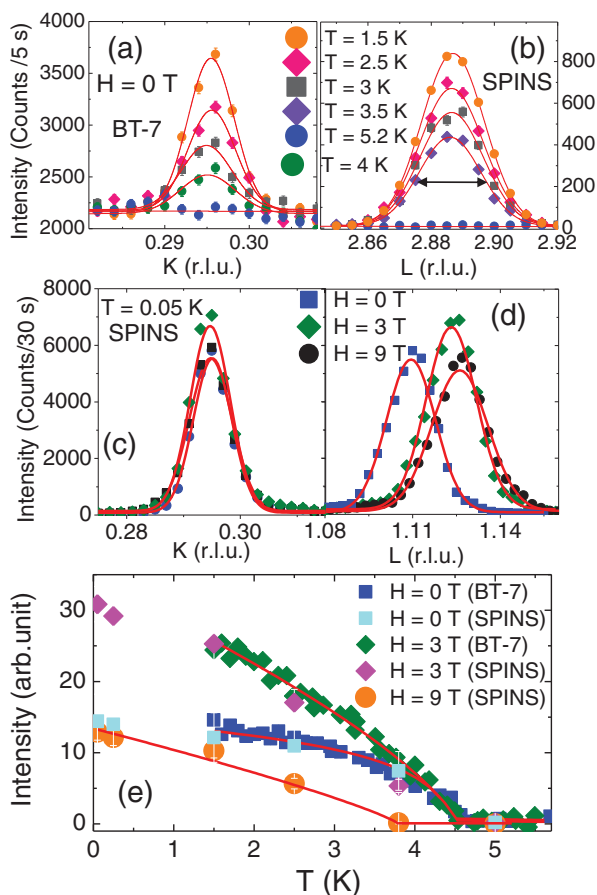


FIG. 1. (Color online) Elastic scattering scans of the type (a) $(0, K, 1.11)$, BT7 measurements, and the (b) $(0, 0.295, L)$, SPINS measurements at various temperatures and zero field. (c) and (d) Elastic scans measured on SPINS at different fields and $T = 0.05$ K. (e) Intensity at the $(0, 0.295, 1.11)$ magnetic peak position at different fields as a function of temperature. It is worth noting that the l value of the magnetic peak position changes with applied field [(Fig. 1(d))]. The field measurements were performed at the actual magnetic peak position. Error bars represent one standard deviation.

positions, while no higher harmonics of incommensurate wave vectors were observed. The best fit of the data is obtained with the Ce spins lying within the basal plane and forming an amplitude-modulated SDW with spins pointing along the b axis. The periodicity of the amplitude modulation is given by the modulation vector $\epsilon = (0, 0, 0.705, 0.11)$ with respect to a simple commensurate structure. The numerically simulated elastic-scattering pattern, depicted with this spin arrangement, is shown in Fig. 2(b). Since there are four equivalent domains for this spin structure, our calculation averages over all four magnetic domains. We see that the calculated cross sections are in good agreement with the experimental data. Some of the weaker satellite peaks, as found in the magnetic structure calculation, were hard to distinguish from the background. Elastic measurements were also performed with the CeAg_2Ge_2 crystal rotated in the (HHL) zone, but no magnetic Bragg peaks were observed in this plane. We determine that the static moment associated with the long-range incommensurate magnetic peaks at $T = 1.5$ K is $M_{\text{Ce}} \simeq 1.23(3)\mu_B$, significantly

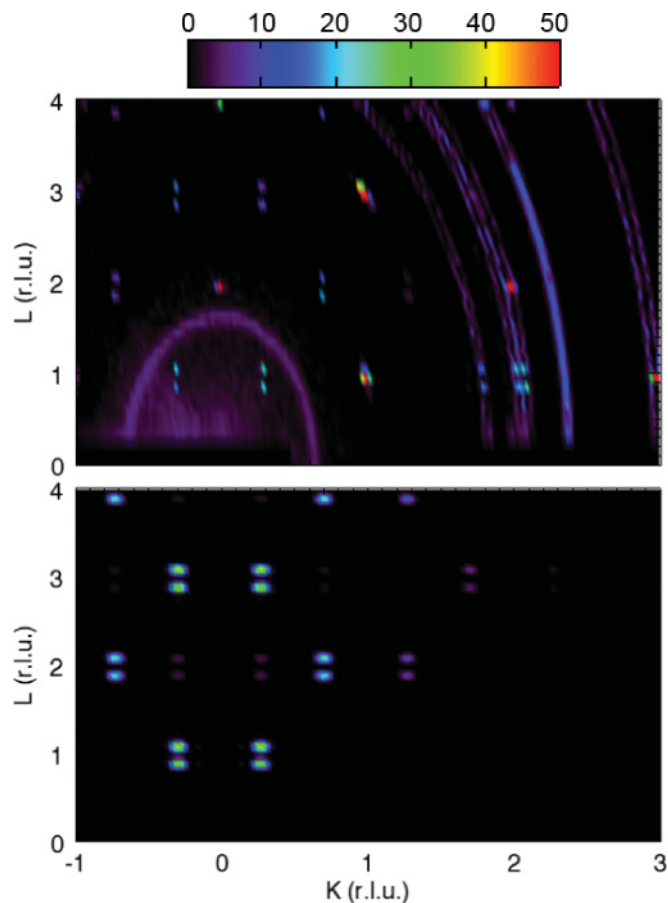


FIG. 2. (Color online) (a) Pattern of elastic intensity at $T = 1.5$ K measured on BT9 in the $(0KL)$ zone. The circles at high and low q arise from the Al powder and ^4He , respectively. (b) Calculated scattering pattern for long-range magnetic order using the spin-density-wave magnetic configuration, which is domain-averaged as described in the text.

smaller than that expected for a fully degenerate $J = 5/2$ ground-state Ce^{3+} ion value of $2.15\mu_B$.

Qualitatively different behaviors are observed in the field-dependent scans. Representative scans at $T = 0.05$ K along K and L directions at $\mathbf{q} = (0, 0, 0.295, 1.11)$ and at different magnetic fields are plotted in Figs. 1(c) and 1(d). The data clearly reveal the movement of the magnetic peak positions along the $[00L]$ direction. The temperature dependence of the magnetic peak intensity at $\mathbf{q} = (0, 0, 0.295, 1.11)$ at different magnetic fields is plotted in Fig. 1(e), which reveals that the magnetic intensity at 3 T is higher compared to 0 or 9 T data. This suggests a fluctuation in the ordering moment as a function of field. Corrections were made in the l value for the field measurements such that \mathbf{q} represents the actual magnetic peak position. Fitting the data to a power law, $I \propto (1 - T/T_N)^{-2\beta}$, yields the AFM transition temperature $T_N \simeq 4.5$ K at $H = 0$ and 3 T. At $H = 9$ T, T_N shifts to lower temperature ($\simeq 3.8$ K). The exponent β at 0 and 3 T are 0.28(2) and 0.34(2), respectively, suggesting three-dimensional interactions.¹⁵

In Figs. 3(a) and 3(b), we have plotted the field-dependent scans of integrated intensities as a function of temperature at magnetic peak position $\mathbf{q} = (0, 0, 0.295, 1.11)$ and

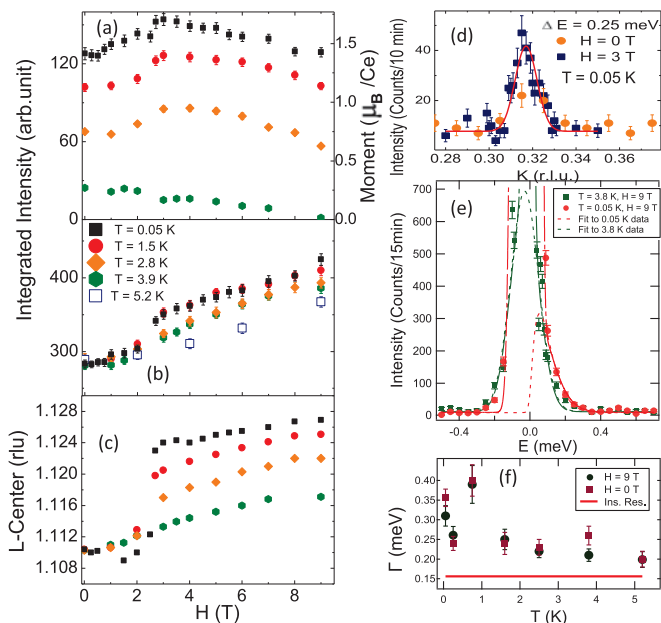


FIG. 3. (Color online) (a) and (b) Variation of integrated magnetic intensity at $(0,0.295,1.11)$ and nuclear intensity at $(0,0,2)$ as a function of field at different temperatures. (c) Change in L-center position of magnetic Bragg peak at $(0,0.295,L)$ as a function of field. An abrupt change is clearly observed at $H = 2.7$ T. (d) Constant-energy scan at $E = 0.25$ meV along K axis at $(0,K,1.115)$ clearly shows enhanced fluctuation at $H = 3$ T field, which is when there is an abrupt change in (a) and (c) as well. (e) Representative inelastic scans at two temperatures and 9 T. (f) Temperature dependence of the observed linewidths (FWHM) at $H = 0$ and 9 T. The incoherent scattering from vanadium was used to determine the energy resolution.

the nuclear peak position $\tau = (0,0,2)$, respectively. We see that the integrated intensity of the magnetic Bragg peak starts increasing as the applied field is increased to 2.7 T, develops a maxima around 3-T field followed by a gradual decrease as the applied field value is increased to 9 T. In terms of the ordered moment, it changes from $1.43\mu_B$ at $H = 0$ T to $1.61\mu_B$ at $H = 2.7$ T to $1.4\mu_B$ at $H = 9$ T at $T = 0.05$ K. This behavior in field continues until $T \simeq 3.8$ K. For $T \geq 3.8$ K, the integrated magnetic intensity continuously decreases as the field is increased. Similar patterns in the change of magnetic intensities were observed at other magnetic peak positions. Interestingly, a substantial induced magnetic moment ($0.23\mu_B$ per Ce ion at $H = 3$ T at $T = 0.05$ K) is observed as additional scattering on the (002) nuclear peak, which monotonically increases with fields. The intensity at the (002) position also increases above $T_N \simeq 4.5$ K as a function of field, thus suggesting that the observed behaviors at magnetic Bragg peaks and $(00L)$ magnetonuclear peaks are decoupled. Measurements were also performed for reverse field sweeps and no hysteresis was observed in the magnetic or nuclear case. The observed increase in the (002) peak intensity is either due to the field-induced alignment of free Ce moments parallel to the field or the induced moment from the intermixing of lower-level crystal-field excitations in applied field, or a combination of both.¹⁶ More research is needed to understand that.

The ordered moment of correlated Ce ions, forming the SDW configuration, exhibits a subtle change in field below $T \leq 3.8$ K. In a notable observation, as shown in Fig. 3(c), we have found that the onset of moment variation at $H = 2.7$ T is accompanied by a discontinuous movement of the SDW propagation vector along the L direction. In reciprocal space, the l value of the magnetic vector changes from $l = 1.11$ at $H = 0$ T to $l = 1.123$ at $H = 2.7$ T and $T = 0.05$ K. As the applied field is increased further ($H \geq 5$ T), the movement of the SDW moderates and tends to settle at higher field values. This coincidence of the change in ordered moment of Ce ions and the discontinuous movement of the underlying SDW in H - T space clearly suggests a coupling between them. At higher fields, the magnetic intensity decreases at all temperatures, which is consistent with the magnetic behavior of the AFM materials. No such behavior was observed at the magnetonuclear peak position (002) .

Several possibilities were explored to explain this unusual coupling, including the effect of field-induced intermixing of low-energy crystal-field levels. Previous measurements^{13,14} of CeAg_2Ge_2 suggested that the crystal-field levels of Ce ions consist of a doublet ground state either degenerate with a doublet first excited state or separated by $\simeq 5$ K. Therefore, the effect of magnetic field perturbation resulting in the intermixing of low lying crystal-field levels cannot be ruled out. This phenomenon, in general, leads to the anti-ferroquadrupolar (AFQ)-type order in magnetic systems with incommensurate wave vectors and is accompanied by higher-order harmonics at low temperatures.¹⁷ Such tendency is also clearly observed in the heat capacity measurements. However, no such indications are found in this case as the SDW magnetic structure of Ce ions remains robust to the lowest measurement temperature and despite repeated efforts, no trace of higher harmonics is observed at low temperature. In addition to that, as shown below in Fig. 4, heat capacity data do not exhibit any anomaly either at $H \simeq 3$ T.

We also performed inelastic measurements. In Fig. 3(d), we have plotted constant-energy scans along $(0,K,1.115)$ direction at an energy transfer $E = 0.25$ meV at $H = 0$ and 3 T.

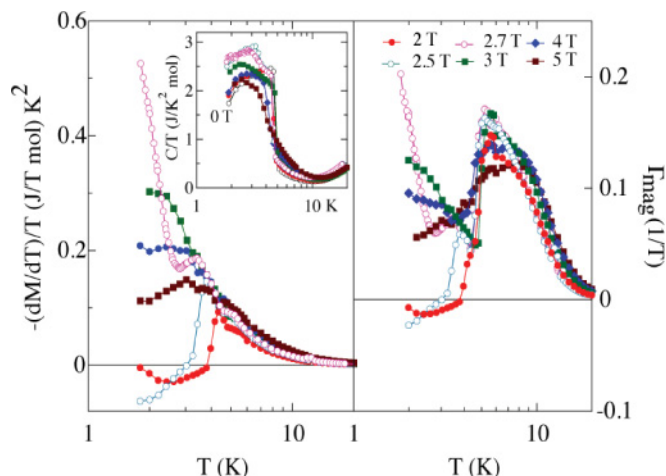


FIG. 4. (Color online) (a) Differential magnetic susceptibility at different fields as a function of temperature. $C(T)/T$ at different fields as a function of temperature are shown in the inset. (b) Variation of Gruneisen ratio parameter at different fields.

Significantly higher intensity is observed at 3 T compared to 0 T data. Fluctuations can lead to the increase or decrease in the magnetic intensity. Resolution-limited Gaussian fit of the 3-T data indicates the dynamic nature of Ce moments with long-range spatial correlation. Representative scans of background-corrected inelastic measurements between $T = 0.05$ and 5.5 K and $H = 0$ and 9 T at the AFM wave vector $\mathbf{q} = (0, 0.295, 1.11)$ are shown in Fig. 3(e). A combination of two Gaussian profiles, representing elastic and quasielastic lines, respectively, multiplied by the detailed balance factor and convoluted with the instrument resolution gives a better fit of the experimental data. At $T = 0.05$ K, the quasielastic line shifts to slightly inelastic position at $E = 0.1$ meV. In Fig. 3(f), we have plotted the estimated linewidths, Γ (FWHM), at different temperatures along with the instrument resolution at $H = 0$ and 9 T. While the estimated linewidths are found to be reasonably broader, ≈ 0.25 meV, than the instrument resolution (0.158 meV), no significant temperature dependence was observed below $T \leq 3.8$ K. The Gaussian approximation of quasielastic data suggests correlated AFM fluctuation of Ce ions.¹⁸ The very weak temperature dependence of the linewidths (increasing with decreasing temperature) can be attributed to the long-range order in CeAg₂Ge₂ with the dominant effect of crystal-field-coupled intersite exchange coupling between Ce ions.¹⁹ Similar behavior has been observed before in long-range ordered magnetic systems where the quasielastic intensity becomes maximum (Γ minimum) as the system passes through the Neel temperature.⁸

Finally, we have performed magnetic Gruneisen ratio measurements to gain more insight into the nature of Ce moment fluctuations in the H - T phase space. The divergence of the Gruneisen ratio parameter defined by the ratio of $-(dM/dT)/T$ and $C(T)/T$, such that $\Gamma_{\text{mag}} = -(dM/dT)/C$, is described as an apt way to check the spin fluctuations.^{1,20} In Fig. 4, we plot the temperature dependence of $-(dM/dT)/T$ [see Fig. 4(a)], $C(T)/T$ [inset, Fig. 4(a)], and Γ_{mag} in Fig. 4(b). While the magnetization was measured

utilizing a high-resolution commercial magnetometer, heat capacity measurements were performed using the relaxation method in a commercial physical-properties-measurement system with magnetic field applied along [100] direction. Two observations are clearly noticeable in this figure: (a) a clear divergence in the ratio Γ_{mag} at $H = 2.7$ T, dominated by the divergence in differential susceptibility, and (b) changes in the slope of Γ_{mag} curves across $H = 2.7$ T and $T \leq 3.8$ K. Although the heat capacity ratio increases sharply at $T \sim 4.5$ K, confirming the magnetic phase transition at $T_N = 4.5$ K, the lack of strong field dependence of $C(T)/T$ in the explored field regime suggests that the electronic density is weakly affected by applied magnetic field in CeAg₂Ge₂. Therefore, the observed linear divergence of Γ_{mag} at $H = 2.7$ T and the changes in the slope of the curves across this field value are magnetic in origin, which are in conjunction with the field-dependent neutron scattering measurements (see Fig. 3).

In summary, we have observed a significant change in the ordered Ce moments as a function of field. The onset of this behavior coincides with the discontinuous movement of intrinsic SDW along L and significant fluctuations along the K direction. It is not yet clear if the observed fluctuation of Ce moments will lead to a quantum phase transition at $T = 0$ K. We point out that the sliding of the SDW is in essence an intrinsic elastic phenomenon.²¹ However, the discontinuous movement of the SDW in CeAg₂Ge₂ suggests a dynamic behavior, accompanied by a finite change in total magnetic energy, which tends to compensate the Ce fluctuations by spatially changing the propagation vector. Previously, Landau had described that a discontinuous change in the magnetic vector involves a change in the total magnetic energy.²² Further understanding of this interesting behavior will require detailed theoretical calculations based on the total energy across the field boundary.

This work used facilities supported in part by the NSF under Agreement No. DMR-0944772.

¹P. Gegenwart, Q. Si, and F. Steglich, *Nat. Phys.* **4**, 186 (2008).

²Q. Si, S. Rabello, K. Ingersent, and J. L. Smith, *Nature (London)* **413**, 804 (2001).

³H. Lohneysen, A. Rosch, M. Vojta, and P. Wolfle, *Rev. Mod. Phys.* **79**, 1015 (2007).

⁴P. Coleman, C. Pepin, Q. Si, and R. Ramazashvili, *J. Phys. Condens. Matter* **13**, R723 (2001).

⁵J. A. Hertz, *Phys. Rev. B* **14**, 1165 (1976).

⁶A. J. Millis, *Phys. Rev. B* **48**, 7183 (1993).

⁷T. Moriya and T. Takimoto, *J. Phys. Soc. Jpn.* **64**, 960 (1995).

⁸W. Knafo, S. Raymond, P. Lejay, and J. Flouquet, *Nat. Phys.* **5**, 753 (2009).

⁹H. Kadowaki, Y. Tabata, M. Sato, N. Aso, S. Raymond, and S. Kawarazaki, *Phys. Rev. Lett.* **96**, 016401 (2006).

¹⁰M. C. Aronson, R. Osborn, R. A. Robinson, J. W. Lynn, R. Chau, C. L. Seaman, and M. B. Maple, *Phys. Rev. Lett.* **75**, 725 (1995).

¹¹O. Stockert, M. Enderle, and H. Lohneysen, *Phys. Rev. Lett.* **99**, 237203 (2007).

¹²S. D. Wilson, P. Dai, D. T. Adroja, S.-H. Lee, J.-H. Chung, J. W. Lynn, N. P. Butch, and M. B. Maple, *Phys. Rev. Lett.* **94**, 056402 (2005).

¹³A. Loidl, K. Knorr, G. Knopp, A. Krimmel, R. Caspary, A. Böhm, G. Sparn, C. Geibel, F. Steglich, and A. P. Murani, *Phys. Rev. B* **46**, 9341 (1992).

¹⁴A. Thamizhavel, R. Kulkarni, and S. K. Dhar, *Phys. Rev. B* **75**, 144426 (2007).

¹⁵A. Pelissetto and E. Vicari, *Phys. Rep.* **368**, 549 (2002).

¹⁶J. G. Lussier, M. Mao, A. Schröder, J. D. Garrett, B. D. Gaulin, S. M. Shapiro, and W. J. L. Buyers, *Phys. Rev. B* **56**, 11749 (1997).

¹⁷T. Onimaru, T. Sakakibara, N. Aso, H. Yoshizawa, H. S. Suzuki, and T. Takeuchi, *Phys. Rev. Lett.* **94**, 197201 (2005).

¹⁸U. Walter, M. Loewenhaupt, E. Holland-Moritz, and W. Schlabit, *Phys. Rev. B* **36**, 1981 (1987).

¹⁹C. Broholm, J. K. Kjems, G. Aeppli, Z. Fisk, J. L. Smith, S. M. Shapiro, G. Shirane, and H. R. Ott, *Phys. Rev. Lett.* **58**, 917 (1987).

²⁰L. Zhu, M. Garst, A. Rosch, and Q. Si, *Phys. Rev. Lett.* **91**, 066404 (2003).

²¹E. Fawcett, *Rev. Mod. Phys.* **60**, 209 (1988).

²²L. D. Landau, *Phys. Z. Sowjetunion* **11**, 26 (1937).